Control of a dual-layer loudspeaker array for the generation of private sound

Mincheol Shin[a)]
Filippo M. Fazi[b)]
Fabio C. Hirono[c)]
Philip A. Nelson[d)]
Institute of Sound and Vibration Research, University of Southampton
University Road, Southampton, SO17 1BJ, United Kingdom

A dual-layer loudspeaker array has been constructed and controlled in order to ensure directional radiation over only one hemisphere of the region surrounding the array. This enables the generation of a "private sound field" for one or a few persons situated in a certain spatial region relative to the array. The paper compares the performance of two conceptually different types of algorithm. The performance of the control algorithms have been compared theoretically and investigated by using computer simulations. The same control algorithms and the simulations have been experimentally verified with the prototype dual-layer array composed of 16 loudspeakers. Excellent agreement between experiment and theory is achieved.

1 INTRODUCTION

There have been several research studies related to acoustic signal control algorithms for the generation of a so called private sound field. The goal of those studies is to develop an acoustic signal control algorithm with a specific sound system whose radiation pattern is sufficiently directional to realise a sound space where only one listener (or a few listeners) can hear sound[1, 2, 3]. Similar technologies, using mulitple source arrays have been investigated for their suitability in generating acoustically *bright* and *dark* zones for the purposes of producing 'personal sound'[4]. Choi et al.[5] and Shin et al.[6] used the concept of control regions associated with bright and dark sound regions. In addition, several private sound field generation techniques have been investigated through the practical implementation of personal audio systems[7, 8].

[a)] M.Shin@soton.ac.uk
[b)] ff1@isvr.soton.ac.uk
[c)] fchirono@gmail.com
[d)] P.A.Nelson@soton.ac.uk

The acoustic problem of generating a private sound space is schematically described in Figure 1. It is defined by two acoustic spaces, the 'audible' and 'inaudible' spaces, which are respectively described by two arcs with angles of θ_b and θ_d on the control circle of radius R that surrounds the array of loudspeakers. The private sound space can be realised by controlling the multiple source inputs to enhance the sound energy radiating into the audible space whilst minimizing the sound energy radiating into the inaudible space. The source array module composed of multiple loudspeakers is assumed to be of a size with the dimensions W and D which are the width and depth of the source array module.

In this paper, the private sound field has been achieved by the use of two conceptually different control algorithms. One is the minimisation control algorithm, based on the least squares method[9, 10], and the other is the maximisation control algorithm, based on the energy difference maximisation method[6]. Those two algorithms are compared in terms of theoretical concepts and their performance verified with simulated and experimental results. The specific sound system used for the verifications mentioned is provided by the dual-layer linear loudspeaker array. The miniaturized array consists of two linear arrays of eight elements positioned back-to-back. This arrangement allows the control of the back radiation from the sound system and thus broadens its range of applications.

This paper begins with the introduction of the algorithms used for the private sound field generation in Section 2. Section 3 shows the design of the implemented real dual-layer loudspeaker array. The results of simulations are presented in the form of polar radiation patterns with the measured transfer functions in Section 4. Experimental validation of the simulated results follows in Section 5 and shows reasonably good matches with simulated results in Section 4. The research is summarised and concluded in Section 6.

2 THEORY

Two radiation pattern control algorithms are exploited in this paper; one is referred to as the least squares minimisation method and the other is referred to as maximisation control and is based on the energy difference maximisation method. The minimisation control algorithms can sometimes suffer from the matrix inversion process which can cause instability in the solutions due to an ill-conditioned plant matrix, the latter being the matrix of source-receiver transfer functions (expressed in the frequency domain). On the other hand, the maximisation control method avoids the matrix inversion process but does not impose a constraint on the phase of the reproduced sound. With the knowledge of these main differences, this paper focuses on the specific performance of these two algorithms used to control radiation patterns of the loudspeaker array.

2.1 Minimisation Control

The minimisation control algorithm used in this paper is a frequency-domain least squares deconvolution[11]. The cost function to be minimised has been defined as the sum of a performance error term, given by the norm of the difference between the target and the reproduced signals, and of an effort penalty term, given by the squared norm of the loudspeaker signal vector, weighted by a positive real regularization parameter, set as Equation (1).

$$J = \left\| \mathbf{Zq} - \mathbf{a} \right\|^2 + \beta \left\| \mathbf{q} \right\|^2, \tag{1}$$

where **Z** is so called plant matrix, the transfer function matrix of the plant, **a** is the vector of target signals at a set of control points (see Figure 3), **q** is the source strength vector, which represent the digital filter coefficients for given frequency, and the β is the Tikhonov regularization parameter. All of these are frequency dependent components so that the notations here are assumed to be at a single frequency.

The parameter β can be varied from zero to infinity, and the corresponding cost function will gradually change from containing only the performance error term to containing only the effort penalty term; therefore, β can be used to control the power output from the loudspeakers at the expense of a higher performance error. This parameter is chosen to be proportional to the norm of the plant matrix (that is its largest singular value), namely

$$\beta = \beta_0 \|\mathbf{Z}\| = \beta_0 \sigma_{\max}, \tag{2}$$

where $\sigma_{\max}$ is the maximum singular value of the transfer function matrix $\mathbf{Z}$, and the parameter β_0 is the real positive constant number for adjusting the β. Finally, the optimal filters are calculated with the following formula,

$$\mathbf{q}_{opt} = \left[\mathbf{Z}^H \mathbf{Z} + \beta \mathbf{I}\right]^{-1} \mathbf{Z}^H \mathbf{a}. \tag{3}$$

2.2 Maximisation Control

The energy difference maximisation control algorithm is also used in this paper for generating the private sound field[6]. The cost function to be maximised has been defined with Equation (4) which represents the energy difference between two acoustic spaces divided by the source energy. The cost function is given by

$$J = \frac{e_1 - \alpha e_2}{e_q} = \frac{\mathbf{q}^{\mathrm{H}} \left(\mathbf{R}_1 - \alpha \mathbf{R}_2\right) \mathbf{q}}{\mathbf{q}^{\mathrm{H}} \mathbf{q}}. \tag{4}$$

The matrix $\mathbf{R}_n$ is the spatially averaged correlation matrix of the elements in the transfer function matrix $\mathbf{Z}$ defined on the *M* control points in the *n*-th acoustic space and is defined as,

$$\mathbf{R}_n = \frac{1}{M} \sum_{k=1}^{M} \mathbf{Z}_k{}^{\mathrm{H}} \mathbf{Z}_k \tag{5}$$

The tuning factor α, which is a positive real number, is inserted in the cost function to enable the adjustment of the relative importance between acoustic energy difference and the efficiency of radiation of the multiple sources into the first acoustic space in which the sound should be audible.

The optimized source strength vector $\mathbf{q}_{opt}$ that maximizes the cost function in Equation (4) can be calculated as the eigen-vector associated with the largest eigen-value of the following eigen-value problem.

$$J\mathbf{q}_{opt} = \left(\mathbf{R}_1 - \alpha \mathbf{R}_2\right) \mathbf{q}_{opt}. \tag{6}$$

Note that matrix $\left(\mathbf{R}_1 - \alpha\mathbf{R}_2\right)$ is Hermitian; therefore its eigen-values are real.

3 DESIGN OF A DUAL-LAYER LOUDSPEAKER ARRAY

Large audio reproduction areas such as public address systems have often used a loudspeaker arrays in order to make directional sound radiation patterns. However, the idea of realizing private listening zones, as described in Figure 1, requires the size of loudspeaker array to be as small as possible[12]. The array should have an inter-element spacing as small as possible to decrease spatial aliasing effects and the total length of the array itself. On the other hand, a small driver will have a poor sound radiation performance especially at low frequencies. To counterbalance these constraints, the chosen driver should have an extended low-frequency range when compared to similar sized models. For this reason, the B1S of HiVi Inc[13] with moving coil drivers 1" metal cone and 2 watt maximum power has been selected as the individual loudspeaker element. The external dimensions of the drivers are 3.6 cm. From this value, a distance of 3.8 cm was then chosen as the inter-element spacing, leaving a small gap of 2 mm between each driver. This spacing would yield a spatial aliasing frequency around 9 kHz for a plane wave propagating to the front of the array[14]. The cabinets were built at the ISVR Mechanics Workshop. These are two rectangular parallelepiped wood cabinets, in which we define the front panel as the face which has the loudspeaker holes, and the back panel as the opposite face. There are eight circular holes on the front panel, spaced 3.8 cm from each other, and all drivers in each cabinet share a single cavity with the internal dimensions of 4 × 3.6 × 30.5 cm, yielding a total cavity volume, 439.2×10^{-6} m^3.

Figure 2 represents the dual-layer loudspeaker array consisting of 16 loudspeakers. The total width, depth and height of the loudspeaker array are 33, 12 and 6 cm. Based on the frequency response data sheet provided by manufacturer, the specific low frequency limit is 100 Hz and a high frequency limit is 20 kHz. Considering the spatial aliasing frequency of approximately 9 kHz defined by the spacing above, this array can be used between 100 and 9000 Hz for generating a private sound field.

4 SIMULATIONS

Both algorithms introduced in section 3 have been applied to the simulation setup designed here, in order to obtain a sound radiation pattern that concentrates the acoustic energy in frontal arc, with an aperture angle $\theta_b = 60°$. Figure 3 represents the simulation setup in order to control the loudspeaker input signal for generating the private sound field described in Figure 1. 72 control points are evenly distributed at every 5° on a circle with 1.5 meter radius. The control points located within the frontal 60° aperture arc are the “bright” control points, represented by red circles, and the others, lying outside of that arc, are the “dark” control points, represented by blue circles.

The signal to be reproduced in the bright zone is filtered through a bank of 16 digital filters (one filter per loudspeaker). These filters represented by the vector $\mathbf{q}_{opt}$ have been calculated in the frequency domain using the two algorithms under consideration. The output of each filter feeds into the corresponding loudspeaker of the array.

The transfer functions between all the loudspeakers and all the control points were measured in the ISVR anechoic chamber in order to consider the electrical and acoustical characteristics of amplifier and all the individual loudspeakers as well as the scattering effect of the designed

enclosure. Some examples of the measured transfer functions between all the loudspeakers and the first control point in front side are represented in Figure 4.

Figure 5 shows the simulated polar radiation patterns resulting from the loudspeaker input signals calculated with the minimisation and maximisation methods, using the simulation setup in Figure 3. Three different colored lines overlaid on Figure 5 represent the averaged radiation patterns within three different ranges of frequencies. The blue line represents the low frequency band from 100 to 800 Hz, the green line the middle frequency band from 800 to 3000 Hz, and the red line the high frequency band from 3000 to 8000 Hz.

The maximisation method results in smaller side lobes and a more directional sound radiation patterns compared with the minimisation method in the overall frequency range. Especially in the middle and high frequency ranges, the maximisation method maintains sufficiently high radiating pressure in the frontal direction, similar to that of the minimisation method, as well as sharper directivity.

The loudspeaker input signals are passed through filters having the frequency domain responses shown in Figure 6. Figure 6 (a) and (b) show the frequency domain representation of the solutions obtained by the minimisation and maximisation methods, respectively. The red dashed lines describe the total power of the all the inputs. The minimisation method shows the distributed energy changes with respect to the frequencies while the maximisation method shows the constant energy distribution in frequency domain.

5 EXPERIMENTS

Figure 7 shows the experimental arrangement for measuring the polar radiation patterns by using the loudspeaker array on a turntable and a condenser microphone which is 1.5 metres away from the centre of the loudspeaker array. Both loudspeaker array and microphone are positioned at the 1.10 metres height. The experiment was conducted in the ISVR Large Anechoic Chamber ($9.15 \times 9.15 \times 7.32$ m^3) which has free-field conditions at frequencies above 80 Hz. Both the speaker array and the microphone were connected to a rack containing four RME ADI-8 DS AD/DA converters and an RME ADI-648 digital interface. The converters were connected via ADAT cable to the digital interface, which was in turn connected via MADI cable to a computer located outside of the Chamber. All the measurements were made using a sampling frequency, 44100 Hz. The same setup was used to measure the plant matrix of the array used for the calculation of the digital filters and for the simulations discussed above.

In Figure 8, the measured polar radiation patterns are directly compared with the simulated results using the overlaid plots depicted with green and blue solid lines, respectively. Good agreement between the simulated and the measured polar patterns have been observed within all frequency bands. Despite the measured transfer functions, the slight misalignments of polar radiation patterns between measured and simulated results, observed at the side lobes of Figure 8 (b), (e) and (f), are likely to be caused by the phase-mismatches among the loudspeakers and variations of the transfer functions in the plant matrix when they are simultaneously activated in the array of loudspeakers. These measurement results strongly support the reliability of the source control algorithms and measured transfer functions in Figure 4.

6 CONCLUSIONS

In order to realise a private sound field, a dual-layer loudspeaker array has been constructed and controlled as described in this paper. A very directional acoustic radiation pattern was achieved, concentrating the sound energy radiation only on the front of the array, using two

control algorithms, based on minimisation and maximisation methods, respectively. The performance of the control algorithms have been theoretically investigated by using computer simulations and experimentally verified with the prototype dual-layer array composed of 16 loudspeakers. The results, based on both simulations and experiments, indicate that the maximisation method gives better performance with respect to the creation of a private sound field, since it provides a more directional sound radiation patter than the minimisation method in the overall frequency range, with smaller side lobes. In addition, the maximisation method shows the constant energy distribution with respect to the frequencies whilst the minimisation method shows the fluctuating energy changes.

7 ACKNOWLEDGEMENTS

This work was partially supported by the Korea Research Foundation funded by the Korean Government [KRF-2008-357-D00198], by the Royal Academy of Engineering (UK) and by the Engineering and Physical Sciences Research Council (UK).

8 REFERENCES

1. R. Jones, “On the theory of the directional patterns of continuous source distributions on a plane surface,” *J. Acoust. Soc. Am.*, **16**(3), 147-171, (1945).

2. J. A. Harrell and E. L. Hixson, "An array filtering implementation of a constant-beam-width acoustic source," *J. Audio Eng. Soc.*, **38**(4), 221-230, (1990).

3. D. L. Smith, “Discrete-element line arrays – Their modelling and optimisation,” *J. Audio Eng. Soc.*, **45**, 949-964, (1997).

4. W. F. Druyvesteyn and J. Garas, “Personal sound,” *J. Audio Eng. Soc.*, **45**, 685–701, (1997).

5. J. Choi and Y. Kim, “Generation of an acoustically bright zone with an illuminated region using multiple sources,” *J. Acoust. Soc. Am*., **111**(4), 1695-1700, (2002).

6. M. Shin, S. Lee, F. Fazi, P. A. Nelson, D. Kim , S. Wang , K. Park and J. Seo, “Maximization of acoustic energy difference between two spaces,” *J. Acoust. Soc. Am*., **128**(1), 121-131, (2010).

7. J. Chang, J. Park and Y. Kim, “Scattering effect on the sound focused personal audio system,” *J. Acoust. Soc. Am.*, **125**(5), 3060–3066, (2009).

8. S.J. Elliott and M. Jones, “Active headrest for personal audio,” *J. Acoust. Soc. Am*., **119**, 2702-2709, (2006).

9. O. Kirkeby and P. A. Nelson, “Reproduction of plane wave sound fields,” *J. Acoust. Soc. Am*., **94** (5), 2992-3000, (1993).

10. P. A. Nelson and S. J. Elliott, *Active Control of Sound*, Academic, New York, (1992).

11. O. Kirkeby, P. A. Nelson, H. Hamada and F. Orduna-Bustamante, “Fast Deconvolution of Multichannel Systems Using Regularization.” *IEEE Trans. on Speech and Audio Proc*., **6**(2), 189-194, (1998).

12. S. J. Elliott, J. Cheer, H. Murfet and K. R. Holland, “Minimally radiating sources for personal audio.” *J. Acoust. Soc. Am.,* **128**(4), 1721-1728, (2010).

13. HiVi Inc. “Overview B1S Full-Frequency”, accessed in 14 December 2011 at 16h32 . URL http://www.swanspeaker.com/asp/product/htm/view.asp?id=119.

14. E. Corteel, R. Pellegrini and C. Kuhn-Rahloff, “Wave field synthesis with increased aliasing frequency.” *Proc. on the 124th Convention of Audio Eng. Soc.*, 7362, Amsterdam, 17~20 May (2008).

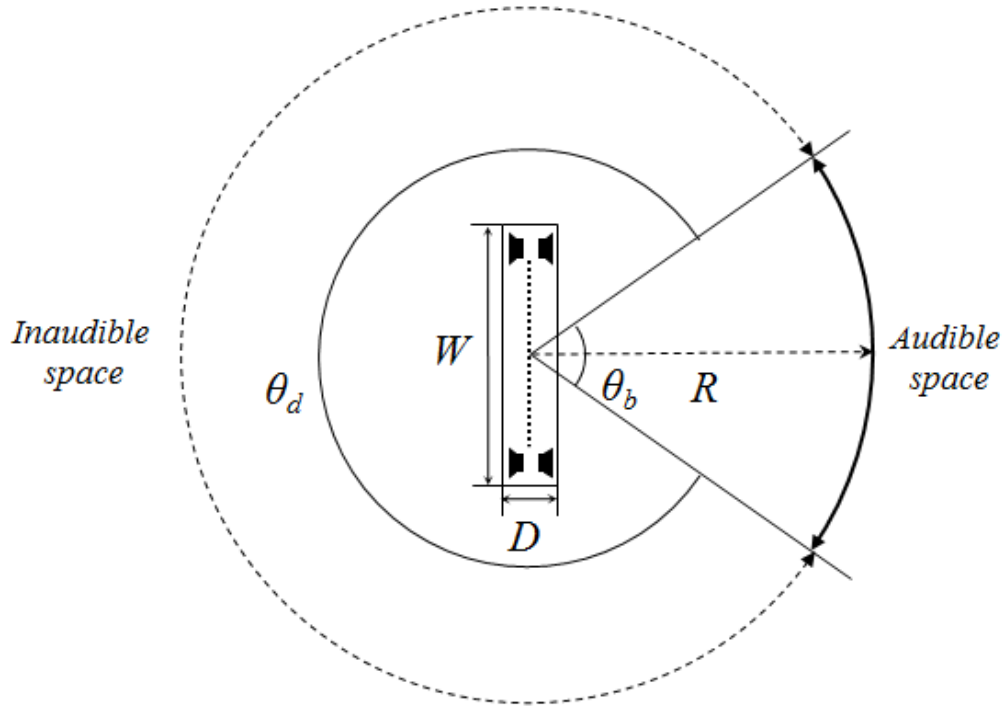

Fig. 1 - Schematic diagram of the private sound field with a dual-layer loudspeaker array

Fig. 2 - Dual-layer loudspeaker array with 16 loudspeakers mounted in an enclosure.

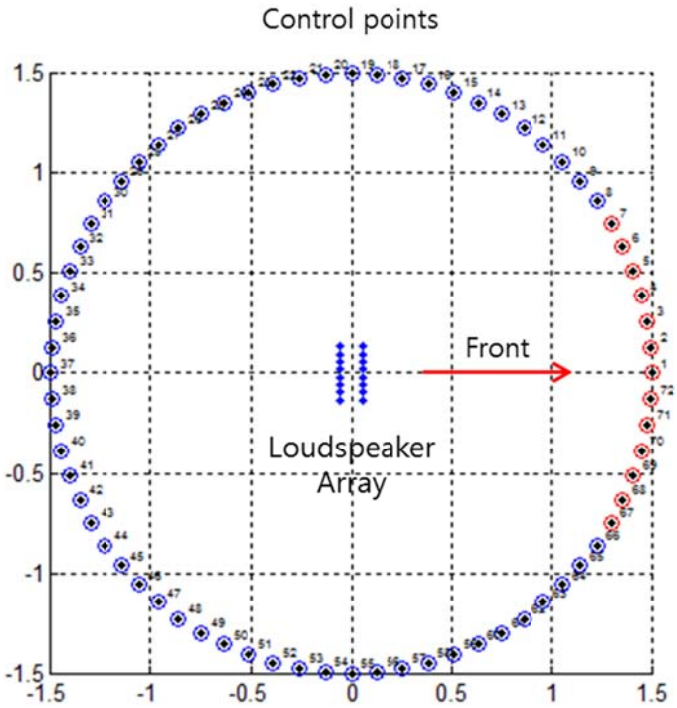

Fig. 3 - Design of the filter calculation and simulation setup. The loudspeakers in the array are represented by blue dots, the control points in the bright zone by red circles and those is the dark zone by blue circles.

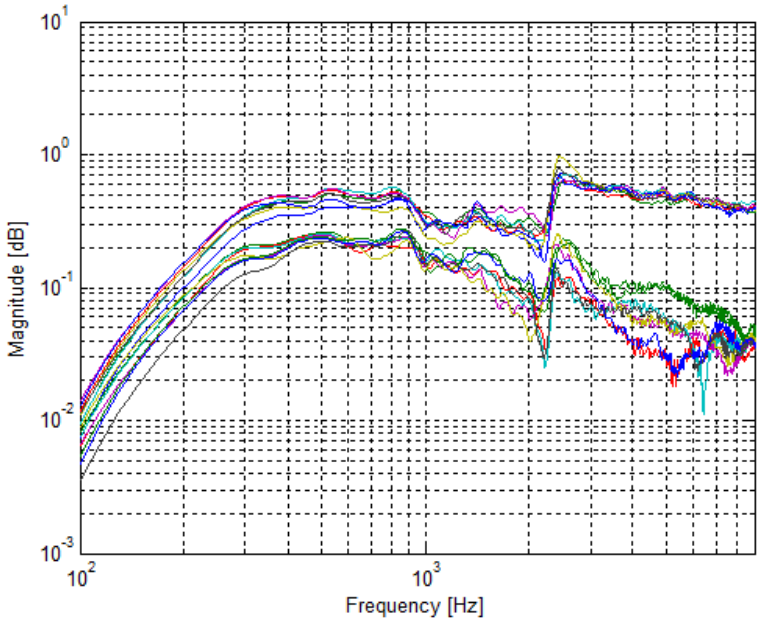

Fig. 4 - Measured transfer functions between the 16 loudspeakers and the control point located at an angle of 0° from the array axis (on-axis).

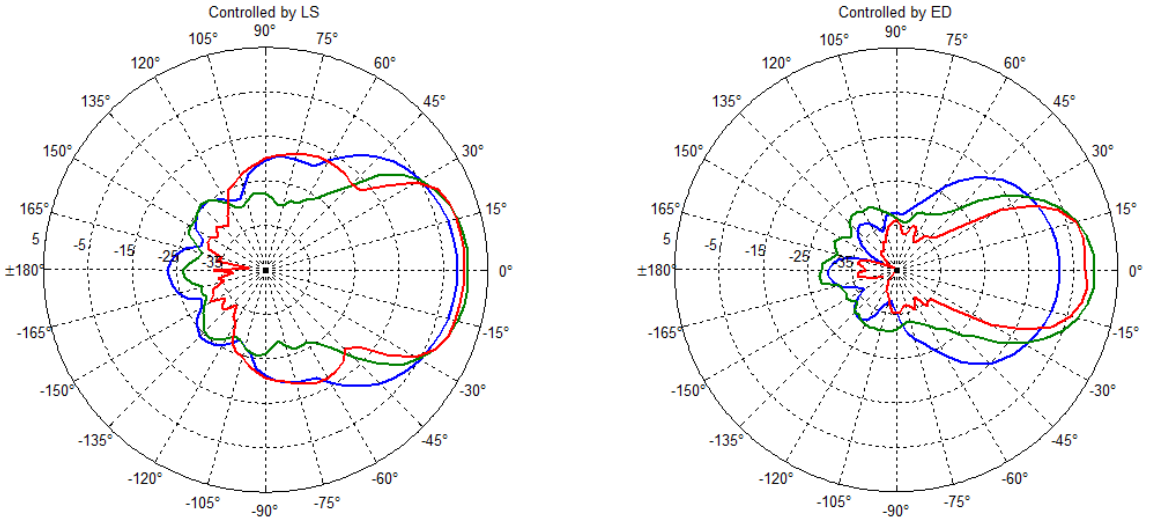

*Fig. 5 - Simulated results with measured transfer function: Frequency-averaged radiation patterns for the low (*100-800 Hz, *blue line), middle (*800-3000 Hz, *green line) and high (*3000 to 8000 Hz, *red line) frequency bands obtained by (a) minimisation and (b) maximisation control methods.*

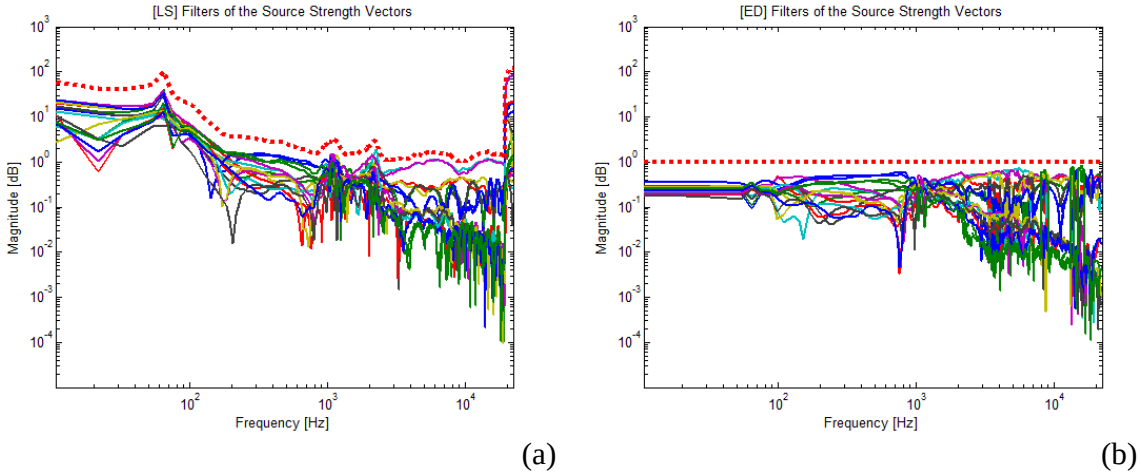

Fig. 6 – Frequency domain filters for the 16 inputs to the dual-layer loudspeaker array controlled by minimisation (a) and maximisation (b) methods.

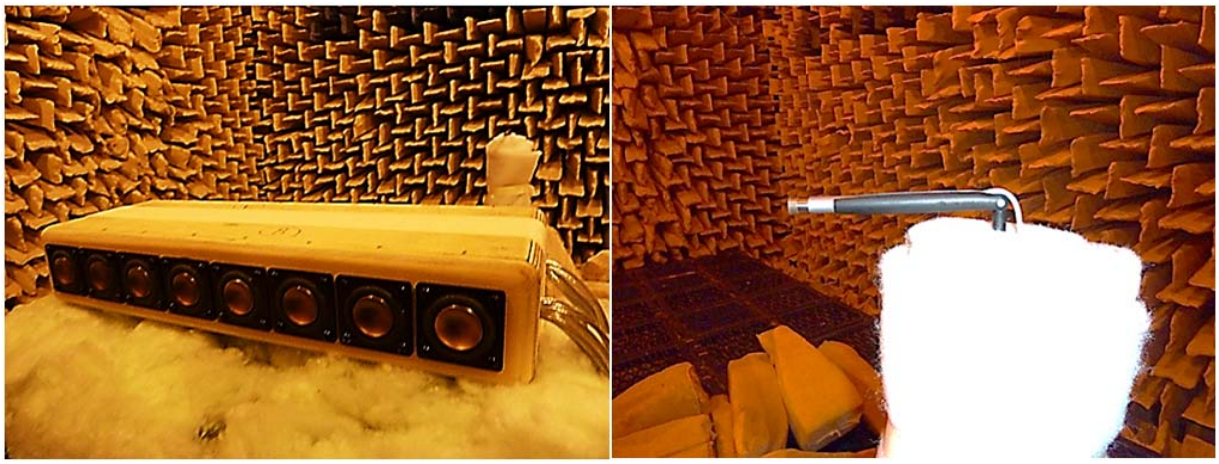

(a) (b)

Fig. 7 - Experimental setup for the measurement of the sound radiation pattern: (a) dual-layer loudspeaker array installed on a turntable in the ISVR anechoic chamber and (b) omnidirectional measurement microphone arranged at 1.5 meter away from the loudspeaker array.

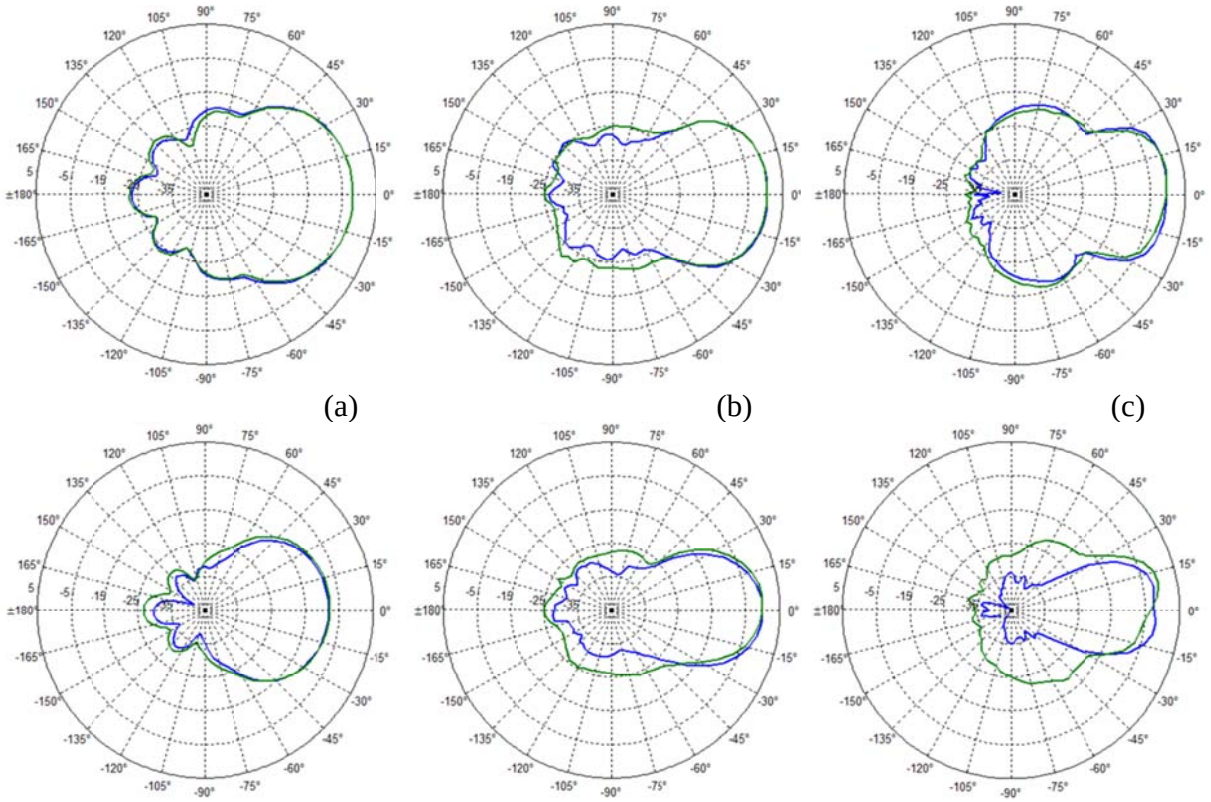

(a) (b) (c)

(d) (e) (f)

Fig. 8 - Measured radiation patterns (green line) compared with the simulated results (blue line, same as in Figure 5) obtained by the minimisation (a, b, c) and maximisation (d, e, f) methods in low (a, d), middle (b, e) and high (c, f) frequency bands.